

Sepiolite-Reinforced Epoxy Nanocomposites: Thermal, Mechanical, and Morphological Behavior

Andrés Nohales,¹ Rafael Muñoz-Espí,² Paula Félix,³ Clara M. Gómez³

¹R&D Department, UBE Corporation Europe SA, Castellón 12080, Spain

²Max Planck Institute for Polymer Research, Mainz 55128, Germany

³Departament de Química Física, Institut de Ciència dels Materials (ICMUV), Universitat de València, Burjassot 46100, Spain

Received 25 February 2009; accepted 15 April 2010

DOI 10.1002/app.32797

Published online 27 July 2010 in Wiley Online Library (wileyonlinelibrary.com).

ABSTRACT: A bisphenol A-based epoxy resin was modified with pristine sepiolite and an organically surface-modified sepiolite and thermally cured using two different curing agents: an aliphatic and a cycloaromatic diamine. The nanocomposites were characterized by dynamic mechanical analysis (DMA), rheology, thermogravimetric analysis (TGA), and electron microscopy. The initial sepiolite-epoxy mixtures show a better dispersion for the sepiolite-modified system that forms a percolation network structure. Mechanical properties have also been determined. The flexural modulus of the epoxy matrix slightly increases by the incorporation of the organophilic sepiolite. The flexural strength of the sepiolite-modified resin cured with the aliphatic diamine increased by 10%,

while the sepiolite-modified resin cured with the cycloaromatic diamine resulted in a lower flexural strength, as compared with the unmodified resin. Electron micrographs revealed a better nanodispersion of the sepiolite in the epoxy matrix for the organophilic modified sepiolite nanocomposite. The initial thermal decomposition temperature did not change significantly with the addition of sepiolite, whereas mechanical properties were affected. The reduced flexural strength was attributed to the stress concentrations caused by the sepiolite modifier. © 2010 Wiley Periodicals, Inc. *J Appl Polym Sci* 119: 539–547, 2011

Key words: sepiolite; epoxy; nanocomposites; surface modification; curing agent

INTRODUCTION

Epoxy resins are, after curing, highly cross-linked amorphous thermoset polymers, extensively used as high-performance protective coatings, structural adhesives, low-stress integrated-circuit encapsulants, and matrix resins for composites. Unfortunately, these highly cross-linked networks are inherently brittle, having limited utility in applications requiring high-fracture toughness. Therefore, it is important to improve toughness without sacrificing the easy processability, high stiffness, heat distortion temperature, and thermal stability.^{1,2} Different pathways have been used for this purpose. On the one hand, properties of epoxy resins can be modified by varying their molecular architectures (especially the crosslink densities) and by changing the curing agent or the monomer.^{1,3,4} On the other hand, the addition of modifiers, such as rubbers,^{1,5} engineering

thermoplastics,^{1,6} or rigid inorganic particles,^{7–26} which form a second phase in the final epoxy matrix, has been a common practice to modify their properties.

Since the work carried out by Toyota Central Research laboratories on polyamide 6/montmorillonite nanocomposites²⁷ and the studies by Giannelis et al.,^{9,28–30} the research area of polymer/clay nanocomposites materials has attracted a great deal of attention.³¹ In this context, polymeric nanocomposites are formed by polymers and dispersed inorganic particles with at least one dimension at the nanoscale (e.g., fibers).²⁸ Thus, the addition of filler particles of nanometric size has become a common practice, because at low nanofiller content, it improves not only the final properties (mechanical, thermal, barrier properties) of the resulting polymer, but also reduces significantly the processing cost.^{7,17,32,33} This improvement depends strongly on the particle content, shape, size, surface characteristics, and degree of dispersion.^{4,7,14,17,33} For instance, the mechanical and thermomechanical properties of composites filled with particles of micrometric size appear to be inferior to those filled with nanoparticles of the same material.¹⁷

Most of the nanocomposites papers based on clays reported in the literature are based on smectite-type

Correspondence to: C. M. Gómez (clara.gomez@uv.es).

Contract grant sponsor: Spanish Ministry of Science and Education (Dirección General de Investigación); contract grant number: MAT2006-03997.

Contract grant sponsor: EU (Program FEDER).

layered silicates, preferentially montmorillonite, due to its highest cation exchange capacity, which easily turns it organophilic. In this work, we study the use of sepiolite, a needlelike-shaped clay, as potential 1D nanofiller for epoxy resins. Sepiolite is a microcrystalline hydrated magnesium silicate, with formula $\text{Si}_{12}\text{O}_{30}\text{Mg}_8(\text{OH},\text{F})_4(\text{H}_2\text{O})_4 \cdot 8\text{H}_2\text{O}$, that exhibits a microfibrillar or needlelike morphology with a particle length of 2–10 μm . Sepiolite is composed of two bands of silica tetrahedrons linked by magnesium ions in octahedral coordination. The discontinuous octahedral layer provides infinite channels along the fiber axis with a cross section of about $1 \times 0.4 \text{ nm}^2$. Structurally, it is formed by an alternation of blocks and cavities (tunnels) that grow up in the direction of the fibers. Its unique structure induces sorptive, colloidal/rheological, and catalytic properties.³⁴ Moreover, due to the lower specific area at the same aspect ratio, fibrous fillers as sepiolite are expected to be better dispersed in the polymer matrices than platelet-like nanofillers as montmorillonite. This results in a matrix with improved rheological properties,^{35,36} mechanical reinforcing capability,^{21,23,35,36} and thermal stability.^{37,38}

Although epoxy nanocomposites have attracted considerable attention in both academia and industry, the great potentiality of fibrous sepiolite as an inorganic modifier remains so far almost unexplored^{38–40} and few articles deal with sepiolite and its surface modification as modifier of epoxy resins.^{24,25} In this sense, the main objective of the present work was to study the influence of the addition of sepiolite and its surface modification upon some selected properties of an epoxy resin cured by using two different amine hardeners. Composite materials containing different percentages of sepiolite were obtained by curing the epoxy matrix. The mechanical, thermal, and morphological behaviors of the resultant composites were investigated to analyze how the nanofiller reinforcing influences the properties of the epoxy matrix. The study would reveal how the surface modification of the sepiolite and/or the amine curing agent (aliphatic or aromatic) influences the final properties of these nanohybrid materials.

EXPERIMENTAL

Materials

The epoxy resin used was commercial diglycidyl ether of bisphenol-A (DGEBA), Araldit GY 250, provided by Vantico (Barcelona, Spain) (187.3 g/eq, hydroxyl/epoxy ratio of 0.122). The curing agents were the diamine-terminated polypropylene oxide Jeffamine D230 (Huntsman Corporation, Pamplona, Spain) and the cycloaromatic diamine 3,3'-dimethylmethylenedi(cyclohexylamine) (MDEA, from Lonza-

cure, Basel, Switzerland). A stoichiometric ratio epoxy/amine, $[\text{E}]/[\text{H}] = 1$, was used along this study. Pristine sepiolite (Pangel S9) and the organophilic sepiolite (Pangel B5), gently supplied by Tolsa (Madrid, Spain), were used as inorganic fillers. The bulk density of these clays is $60 \pm 30 \text{ g/L}$ and the BET surface area is $320 \text{ m}^2/\text{g}$. The average dimensions of the individual sepiolite fibers are 1–2 μm in length and 20–30 nm in diameter (i.e., the aspect ratio is within the range of 100–300). Pangel B5 is an organophilic sepiolite with a cation exchange capacity of 10–15 meq/100 g, obtained by modifying the hydrophilic surface of pristine sepiolite (Pangel S9) with dimethyl benzyl hydrogenated tallow ammonium chloride to increase the compatibility with low-polar polymers.

Preparation of the nanocomposites

The unmodified epoxy resin was prepared by mixing the epoxy prepolymer (DGEBA) with the stoichiometric amount of the curing agent at 75°C with Jeffamine D-230, and at 90°C with MDEA, outgassing the liquid mixture under vacuum, and pouring immediately the mixture into molds. To prepare the sepiolite modified epoxy resin, the dried sepiolite (different grams amount of sepiolite per hundred grams of epoxy monomer, phr) was slowly added to the required amount of epoxy prepolymer and then dispersed in the epoxy prepolymer by using a high-speed mixer Dispermat® CN20 (VMA-Getzmann GmbH), operated for 25 min at 7100 rpm with a 5-cm-diameter disk. The mixture was completely degassed under vacuum at 75°C, and the curing agent was slowly added at the corresponding temperature. Plates were obtained by casting the mixtures into molds consisting of two rectangular glass plaques spaced by a 5-mm Teflon frame and held together with clamps. The plaques were previously covered with a release mold agent (Fretoke NC-44).

Two different curing cycles were used depending on the curing agent to attain maximum conversion degree. That is, 3 h at 75°C and 12 h at 110°C for Jeffamine D230; and 4 h at 130°C, 4 h at 160°C, and 6 h at 180°C for MDEA. The cured plates were cooled down slowly to room temperature, removed from the mold, and cut to produce specimens for mechanical testing. Dynamic differential scanning calorimetry (DSC) measurements for all samples confirmed the completeness of the curing process, as no residual heat was detected after a dynamic temperature scan.

Characterization

Mechanical characterization

Rheological characterization of non-reacted epoxy suspensions was carried out on an AR1000

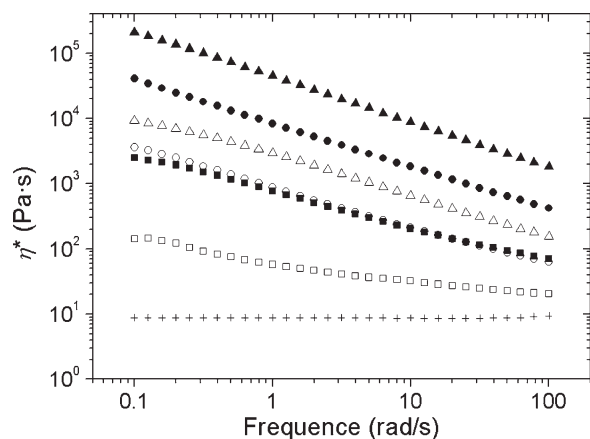


Figure 1 Frequency dependence of the viscosity for epoxy dispersions containing different percentages of unmodified (S9) and organophilic modified (B5 sepiolite: (□) S9 at 2.5 phr, (○) S9 at 5.0 phr, (Δ) S9 at 7.5 phr, (■) B5 at 2.5 phr, (●) B5 at 5.0 phr, (▲) B5 at 7.5 phr, and (+) epoxy prepolymer.

rheometer (TA Instruments) using parallel plates (25 mm in diameter) at 25°C. The thickness of the samples was about 1.0 mm. Dynamic mechanical analysis (DMA) of both unmodified and modified resins were performed on a 2980 Dynamic Mechanic Analyzer (TA instruments) operated in the three-point bending mode at 1 Hz, with an amplitude of 30 μm , and at a scan rate of 3°C/min. At least three tests were carried out for each case. Flexural properties were measured by using three-point bending experiments (3PB) according to the ASTM D790 protocol⁴¹ on an Instron 5582 Universal Tester at $23 \pm 2^\circ\text{C}$ and crosshead displacement rate of 5 mm/min. Fracture toughness experiments were conducted using single edge notched bend specimens according to ASTM E-399 protocol to determine the critical stress intensity factor (K_{IC}) and the critical strain energy release rate (G_{IC}).²⁵

Thermal characterization

Thermogravimetric analysis (TGA) was performed in a TGA Perkin Elmer 7 microbalance under argon atmosphere (100 mL/min) and a heating ramp of 5°C/min.

Morphological characterization

Scanning electron micrographs were recorded for gold-coated, ambient fractured surfaces on a Hitachi S-4100 microscope. The acceleration voltage was set at 10 kV, and the working distances used ranged between 12 and 14 mm. Transmission electron microscopy (TEM) was carried out in a Jeol TEM operated at an acceleration voltage of 100 kV. The specimen was cut from a composite block using an

ultramicrotome, Reichert-Jung Ultracut-E, equipped with a diamond knife. A thin specimen of 80 nm was cut from a sample of about $1 \times 1 \text{ mm}^2$. It was collected in a trough filled with water and placed on a 200-mesh copper grid.

RESULTS AND DISCUSSION

Rheological measurements were carried out to investigate the state of the initial epoxy/sepiolite dispersions. Figure 1 plots the dependence of dispersions viscosity on the frequency at room temperature. For the unmodified epoxy, the viscosity is independent of frequency as expected of a Newtonian fluid. However, the sepiolite modified systems show a clear dependence on frequency more accentuated as the sepiolite concentration increases and also for the modified sepiolite. An increase of four orders of magnitude is observed for the organically modified sepiolite, which means a higher amount of individually dispersed organophilic sepiolite fibers compared to the unmodified one, and thus a better dispersion of the sepiolite nanoparticles.^{35,36} These results point toward the formation of a percolated structure probably due to the interconnection of the sepiolite nanoparticles through van der Waals interactions.

Flexural tests at room temperature were performed to evaluate the stiffness and strength of sepiolite modified epoxy systems cured with two different curing agents. Figure 2 shows typical stress-strain curves for the epoxy resins modified with different contents of the sepiolites S9 and B5, and cured with Jeffamine D230 (panels a and b) and MDEA (panels c and d). These graphs show an initial region with elastic behavior, in which the relationship between the stress and the strain is lineal (Hook's law), and another one with a clear plastic behavior that does not follow this relationship. The mechanical behavior at high stresses is much more plastic for Jeffamine D-230 than for MDEA. This can be explained by the higher degree of freedom of the Jeffamine D-230 chemical structure when compared with the MDEA molecule, which allows the proper alignment of the Jeffamine molecules at high tensions, resulting in the plastic deformation in the direction of the applied tension.^{10,14,15} Addition of sepiolite modifies the curves, and the effect is more accentuated in presence of the surface-functionalized sepiolite. The elastic module increases when increasing the sepiolite concentration, whereas the plastic behavior of the material decreases progressively. The increase in the elastic module is caused by the introduction of rigid inorganic particles, with a higher module than the epoxy matrix. The reduced plasticity of the modified resins can be attributed to the stress concentrations caused by the sepiolite

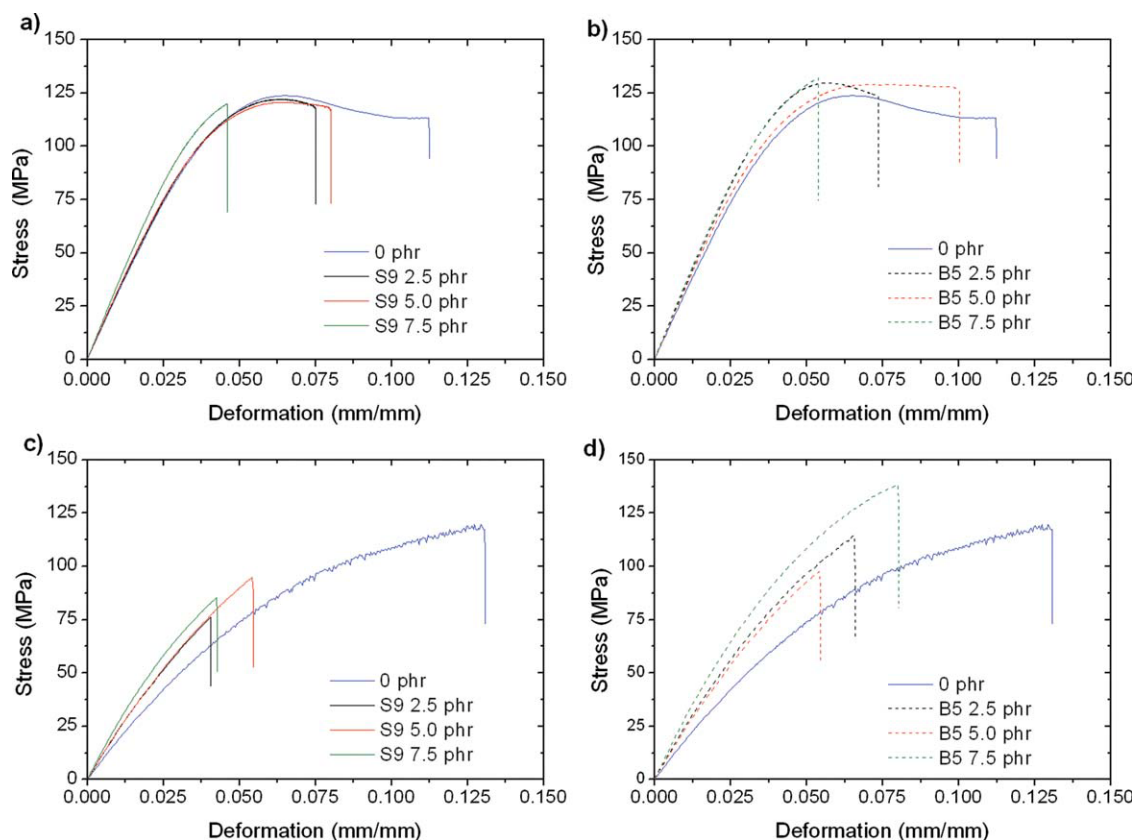


Figure 2 Typical stress-strain plots for the unmodified and sepiolite modified epoxy resin cured with: (a and b) Jeffamine D230 and (c and d) MDEA. [Color figure can be viewed in the online issue, which is available at www.interscience.wiley.com.]

modifier. The improvement in the results is comparable to those reported when using montmorillonite, graphite platelets or sepiolite as fillers.^{4,10,11,16,18–25} The flexural modulus (E), the flexural strength (σ_f), and the deformation at break (ϵ %) were calculated from the stress versus strain curves. Table I compiles the average properties obtained from five of these tests. Irrespective of the curing agent used, the flexural modulus of the resin slightly increases by the incorporation of the sepiolite. Overall, the flexural strength increases and the deformation at break decreases upon addition of sepiolite, being more accentuated for the system cured with MDEA and modified with surface-functionalized sepiolite.

The interactions at the interface matrix/nanofiller play a very important role in results obtained by thermodynamomechanical analysis. During such analysis, polymeric materials can show transitions of different intensity related to the relaxation of the different segments of the polymer chain. The main relaxation ($\tan \delta$), showing the highest intensity, corresponds to the glass transition temperature (T_g). Variations of the intensity and temperature in the value of $\tan \delta$ are representative of the mechanism of molecular dissipation in the macromolecules during the glass transition. The parameters determined

by DMA are, indeed, intimately related with the morphology and microstructure of the nanocomposite, allowing the characterization of the effect of sepiolite on the mobility of the macromolecules of the cross-linked material.

Figure 3 shows the values of the storage module and $\tan \delta$ versus temperature for different concentrations of sepiolite cured with Jeffamine D-230. Similar

TABLE I
Flexural Strength Results Measured for the Systems Under Study

		phr	E (GPa)	σ (MPa)	ϵ (%)
D-230	S9	0	3.08 ± 0.03	113 ± 1	12 ± 1
		2.5	3.18 ± 0.01	122 ± 2	7.9 ± 0.8
		5.0	3.30 ± 0.02	124 ± 3	5.8 ± 0.8
		7.5	3.54 ± 0.01	123 ± 2	7.9 ± 0.7
	B5	2.5	3.38 ± 0.03	122 ± 4	8 ± 1
		5.0	3.32 ± 0.08	127 ± 4	9 ± 3
		7.5	3.48 ± 0.01	132 ± 7	6 ± 1
MDEA	S9	0	2.09 ± 0.02	125 ± 9	12 ± 3
		2.5	2.31 ± 0.01	77 ± 7	4.1 ± 0.5
		5.0	2.36 ± 0.01	95 ± 12	5.4 ± 1.1
		7.5	2.64 ± 0.01	87 ± 9	4.4 ± 0.7
	B5	2.5	2.47 ± 0.02	115 ± 7	6.8 ± 0.7
		5.0	2.45 ± 0.04	106 ± 7	5.8 ± 0.6
		7.5	2.87 ± 0.03	137 ± 11	8 ± 1

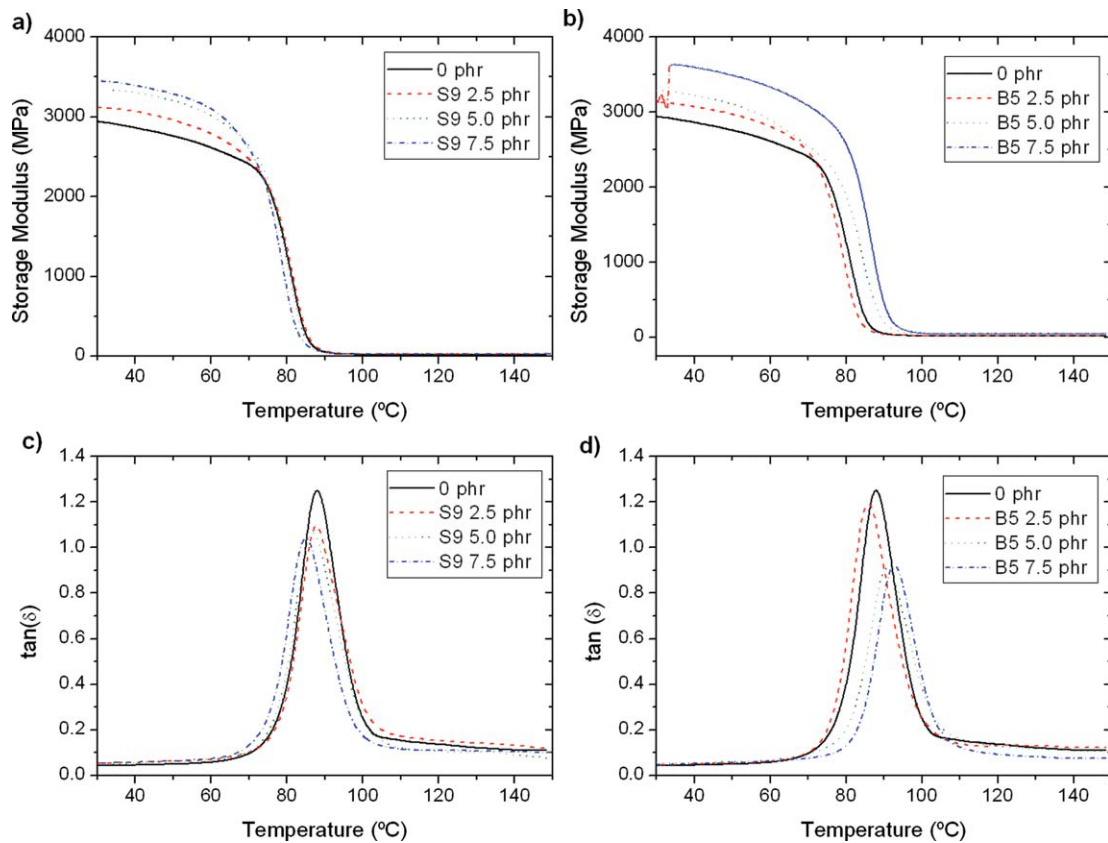


Figure 3 Dynamic mechanical properties of the unmodified and sepiolite modified epoxy resin cured with Jeffamine D230. [Color figure can be viewed in the online issue, which is available at wileyonlinelibrary.com.]

curves are obtained for the systems cured with MDEA. The results obtained can be perfectly correlated with those of the static flexion tests. The storage modulus increases as increasing the sepiolite concentration, and this effect is stronger for the system cured with MDEA, as previously stated. As the temperature increases, the thermal energy of the system increases, and the values of E' decrease progressively, due to the easiest in the mobility of the macromolecules, until temperatures close to the T_g of the materials; at this temperature, E' suffer a drastic decrease. The increase of the modulus in the presence of sepiolite is much higher at temperatures over T_g than at room temperature. These results confirm that the increase of rigidity due to the nanofiller is more effective in less rigid matrices.^{9,15,16,18} For the system with the surface-functionalized sepiolite, T_g slightly increases when curing with Jeffamine D230 and remains practically constant when curing with MDEA. The decrease in the height of $\tan \delta$ is more noticeable for Jeffamine D230, which indicates stronger interactions.^{15,18,21,23} Increased glass transition temperatures have been reported for some nanocomposite systems, while in others a constant or slightly decreased T_g have been found.^{15–18} A decrease indicates that it is not an “adsorbed silicate” effect, as this usually should increase the glass

transition temperature due to chains being tied down by the silicate surface. The presence of sepiolite has little effect on the value of the glass transition temperature, whereas the increase in modulus is more significant.

Typical linear load-displacement curves of 3PB tests have been obtained for the neat epoxy and its nanocomposites. All the samples fail in a characteristic brittle feature, as evidenced by an abrupt rupture without any yield. For both curing agents, the load to break the material increases as the sepiolite concentration increases. Maximum loads are used to calculate the fracture toughness of the samples. Then, values of the critical stress intensity factor (K_{IC}) and the critical strain energy release rate (G_{IC}), which determines the toughness of these brittle materials, are presented in Figure 4. The values of K_{IC} and G_{IC} increase systematically with the introduction of sepiolite. For all concentrations, these values are higher than those of the unmodified system, about 40% for K_{IC} and 60% for G_{IC} . Moreover, toughness increase is slightly higher for the surface-functionalized sepiolite nanocomposites than for the non-modified one. This can be related to a better dispersion and intercalation of the bundles of the surface-functionalized sepiolite within the epoxy matrix.^{19,20,22,23}

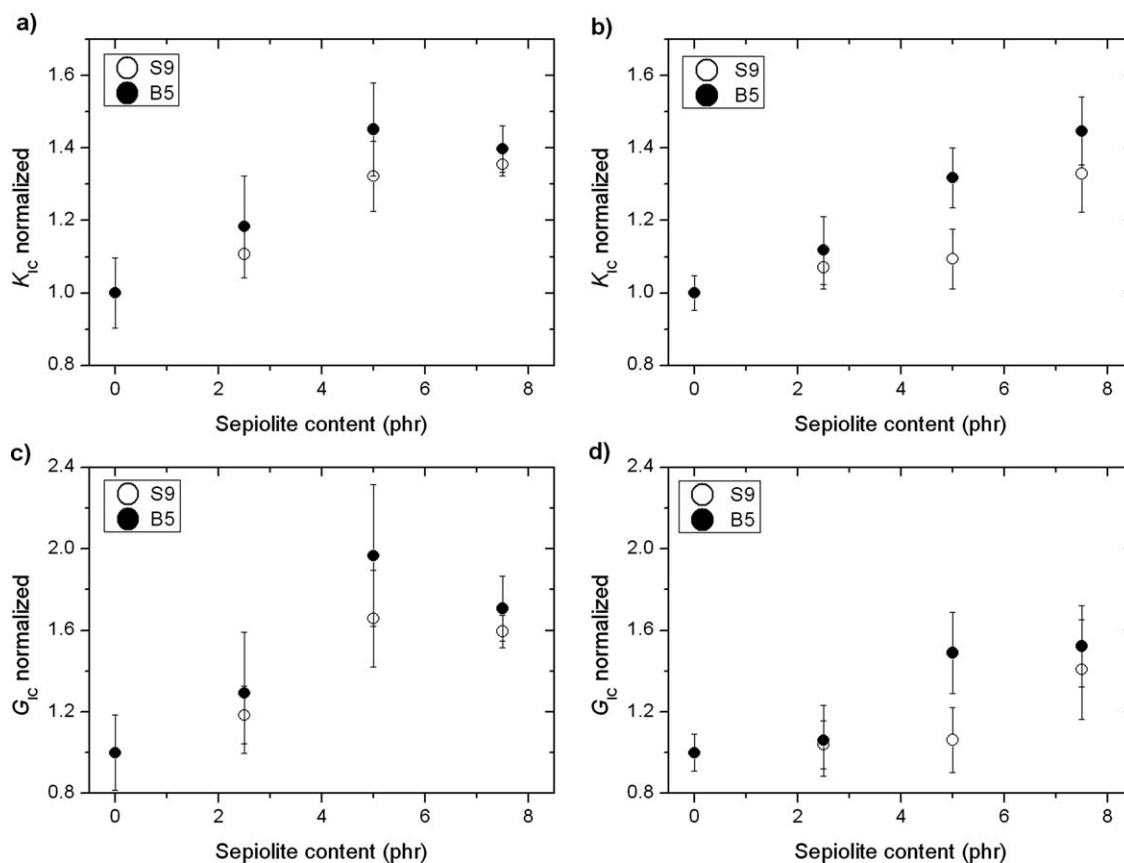


Figure 4 Normalized values of the critical stress intensity factor, K_{IC} , and the critical strain energy release rate, G_{IC} , for the unmodified and sepiolite modified epoxy resin cured with: (a and c) Jeffamine D230 and (b and d) MDEA.

For pure epoxy, the fracture surface was smooth, typical of a glassy material with brittle failure.¹⁵ In contrast, as can be seen in the scanning electron micrographs of Figure 5, the specimens containing sepiolite showed a considerable fracture surface roughness. In case of the systems modified with the surface-functionalized sepiolite, a much rougher fracture surface is seen upon adding sepiolite into the epoxy matrix similar to other epoxy/clay systems.^{10,11,22,33} This is attributed to the fact that the epoxy molecules swallowed the surface-modified sepiolite and had a good interface with the needles of the sepiolite. The untreated sepiolite nanocomposites show a typical fracture topology of filler composites with agglomerates visible in different sizes. The particles are debonded from the resin, and voids are formed around the particles due to the poor compatibility, and the low adhesive strength of the interface between the epoxy, and the untreated sepiolite. The roughness of the surface can be related to the rupture tension.²⁶ The fracture surface of epoxy/sepiolite nanocomposites shows a massive shear deformation. Energy is absorbed leading to the increase in K_{IC} and G_{IC} . The increased surface roughness implies that the path of the crack tip is distorted because of the

sepiolite needles, making crack propagation more difficult.

According to Griffith's theory,¹³ the crack propagates when the released deformation energy creates a new surface of fracture. The formation of a crack or growth of an existing one takes only place if the energy of the process originates a decrease in the total energy (or if the total energy remains constant). Thus, the rupture tension increases when the area of the surface of fracture increases.²⁶ The increase in the tension energy of the crack (applied tension plus released elastic energy) is sufficient to overcome the surface energy of the material. The tenacity increases, consequently, due to a higher adhesion of the organophilic sepiolite particle to the matrix. The presence of the reinforcement would force the crack to progress along a more tortuous path, increasing the fracture surface area. The individual silicate fibers are extremely strong and are unlikely to break during the crack growth. The lower magnification picture shows bright spots corresponding to small bundles of sepiolite fibers. SEM micrographs in Figure 5 show a combination of shear cups and coarse features with debonding between matrix and sepiolite at different locations. It can be assumed that sepiolite is debonded from the epoxy matrix under

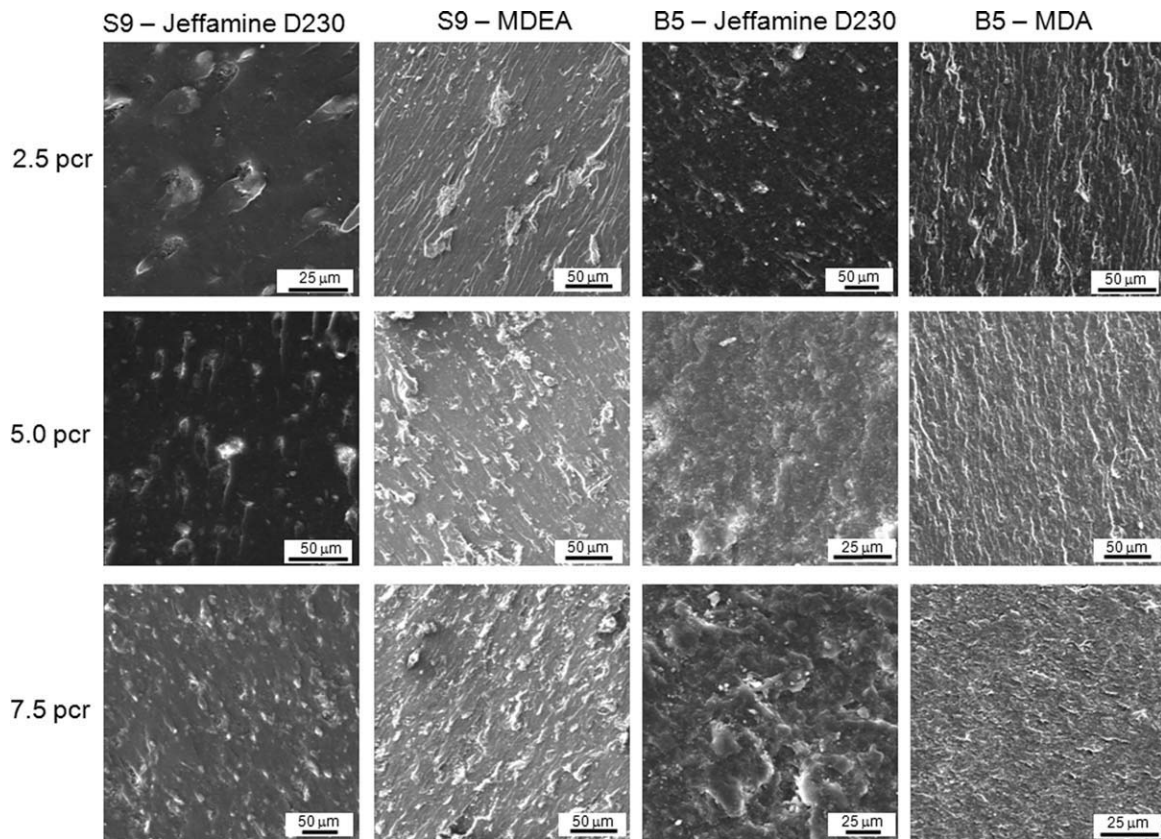


Figure 5 SEM images of epoxy/sepiolite samples.

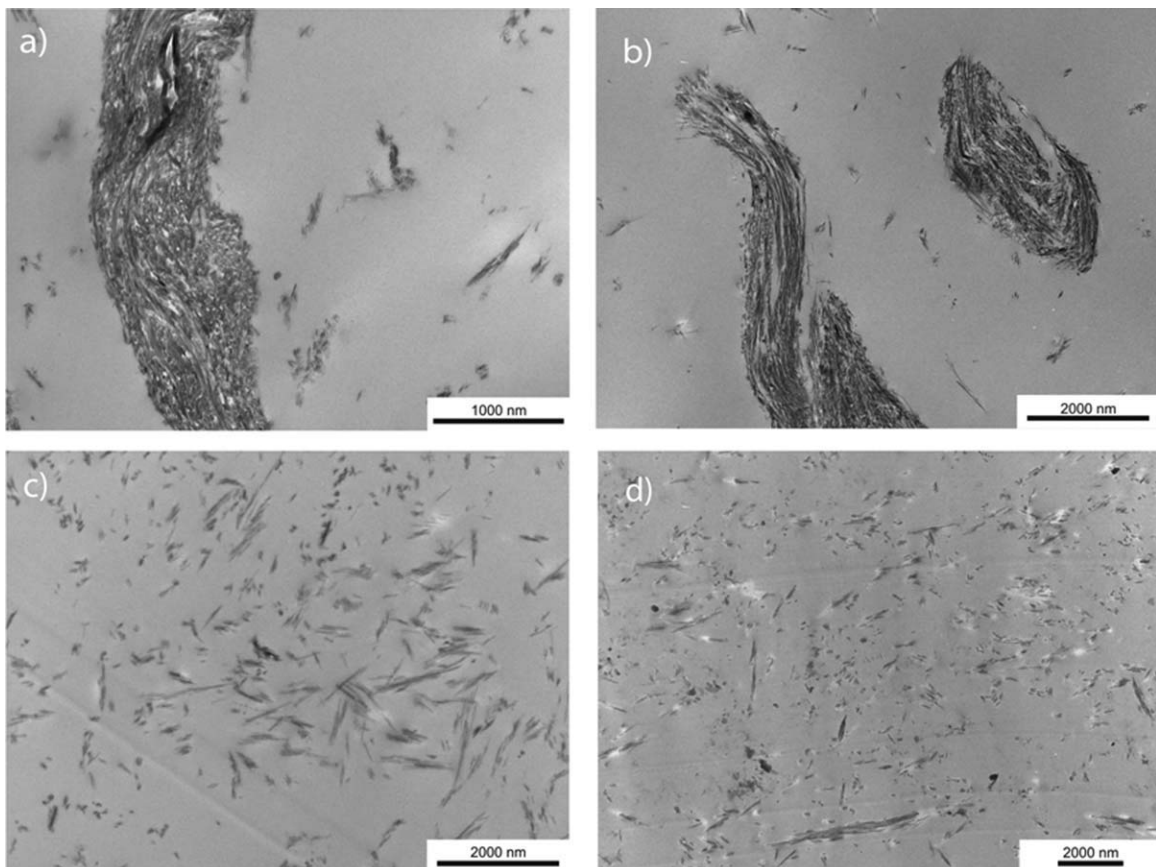


Figure 6 TEM images of epoxy/sepiolite samples: (a) S9 5phr D230, (b) S9 5 phr MDEA, (c) B5 5 phr D230, and (d) B5 5 phr MDEA.

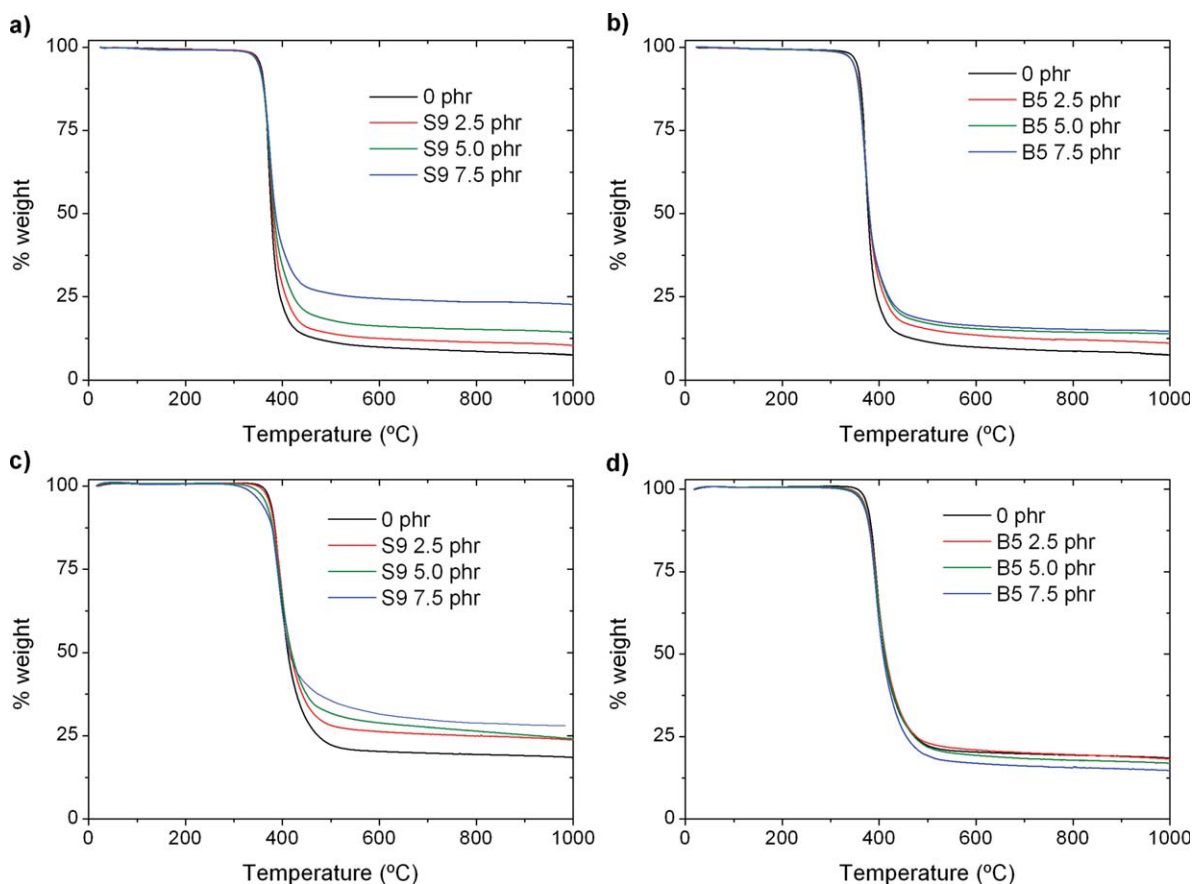


Figure 7 Thermogravimetric analysis of the unmodified and sepiolite modified epoxy resin cured with Jeffamine D230 (a and b) and with MDEA (c and d). [Color figure can be viewed in the online issue, which is available at www.interscience.wiley.com.]

loading and generate microcracks, which upon further loading join to form a single dominant crack. These images present small aggregates of sepiolite (more accentuated for the untreated sepiolite), indicating that the individual fibers are not fully dispersed in the epoxy matrix.

The structure of the cured samples was further studied by transmission electron microscopy (TEM). Figure 6 shows TEM micrographs for the epoxy systems cured with the two curing agents and modified with 5.0 phr of the pure and the surface-functionalized sepiolite. For the non-modified sepiolite, the clay needles are not uniformly distributed, and large regions of pure epoxy are observed. The micrographs show large inorganic aggregates, which may be responsible of the tails, observed in the SEM images of the fracture. A closer observation reveals that the aggregates are comprised of several sepiolite fibers sticking together to build up bundles of fibers which can themselves form agglomerated structures. Contrarily, the organophilic sepiolite B5 shows a more uniform dispersion without large aggregates.

The thermal stability of composites was determined by TGA. Figure 7 contains the TGA curves of the unmodified and sepiolite modified epoxy cured

using the two different curing agents (panels a and b for D230 and panels c and d for MDEA). All systems exhibit thermal degradation and significant weight loss with temperature. In addition, the thermal degradation always occurs in one-step. The peak degradation temperature was determined from the first derivative of the TGA curve, respectively. The onset and the end set of thermal degradation temperature were determined from the intersection of two tangents. The initial thermal decomposition temperature did not change significantly with the addition of sepiolite and was very similar for the two cured systems. The higher the values are, the higher is the thermal stability. The highest char content corresponds to the highest modified system.

CONCLUSIONS

Morphological, flexural, and thermal properties of a bisphenol A-based epoxy resin modified with untreated sepiolite Pangel S9 and surface modified sepiolite, Pangel B5, and cured using an aliphatic and a cycloaliphatic diamine were determined experimentally. DMA data revealed slightly

influence of the sepiolite on the glass transition temperature, while the modulus in the glassy state increases compared with the unmodified resins. The morphology of the cured samples, as seen by SEM and TEM, shows that a complete separation of the sepiolite fibers was not attained; small bundles of fibers are seen. The flexural modulus of the epoxy resin slightly increases by the incorporation of the organophilic sepiolite. The flexural strength show about a 10% increase for the modified resin cured with D230. All systems exhibit thermal degradation and significant weight loss with temperature in one step that is not significantly altered by the presence of sepiolite.

References

- Pascault, J. P.; Sautereau, H.; Verdu, J.; Williams, R. J. J. *Thermosetting Polymers*; Marcel Dekker: New York, 2002.
- May, C. A. *Epoxy Resins. Chemistry and Technology*, 2nd ed.; Marcel Dekker Inc.: New York, 1998.
- Blanco, M.; Corcuera, M. A.; Riccardi, C. C.; Mondragon, I. *Polymer* 2005, 46, 7989.
- Kornmann, X.; Lindberg, H.; Berglund, L. A. *Polymer* 2001, 42, 4493.
- Moschiar, S. M.; Riccardi, C. C.; Williams, R. J. J.; Verchere, D.; Sautereau, H.; Pascault, J. P. *J Appl Polym Sci* 1991, 42, 717.
- Hodgkin, J. H.; Simon, G. P.; Varley, R. J. *Polym Adv Technol* 1998, 9, 3.
- Pinnavaia, T. J.; Bell, G. W., Eds. *Polymer-Clay Nanocomposites*; Wiley: New York, 2000.
- Zilg, C.; Mülhaupt, R.; Finter, J. *Macromol Chem Phys* 1999, 200, 661.
- Vaia, R. A.; Teukolsky, R. K.; Giannelis, E. P. *Chem Mater* 1994, 6, 1017.
- Zerda, A. S.; Lesser, A. J. *J Polym Sci Part B: Polym Phys* 2001, 39, 1137.
- Liu, W. P.; Hoa, S. V.; Pugh, M. *Compos Sci Technol* 2005, 65, 307.
- Becker, O.; Varley, R.; Simon, G. *Polymer* 2002, 43, 4365.
- Miyagawa, H.; Foo, K. H.; Daniel, I. M.; Drzal, L. T. *J Appl Polym Sci* 2005, 96, 281.
- Lan, T.; Pinnavaia, T. J. *Chem Mater* 1994, 6, 2216.
- Ratna, D.; Manoj, N. R.; Varley, R.; Singh Raman, R. K.; Simon, G. P. *Polym Int* 2003, 52, 1403.
- Ye, Y.; Chen, H.; Wu, J.; Ye, L. *Polymer* 2007, 48, 6426.
- Komarneni, S. *J Mater Chem* 1992, 2, 1219.
- Pervin, F.; Zhou, Y.; Rangari, V. K.; Jeelani, S. *Mater Sci Eng A* 2005, 405, 246.
- Bozkurt, E.; Kaya, E.; Tanoglu, M. *Compos Sci Technol* 2007, 67, 3394.
- Wang, K. E.; Chen, L.; Wu, J.; Toh, M. L.; He, C.; Yee, A. F. *Macromolecules* 2005, 38, 788.
- Yasmin, A.; Daniel, I. M. *Polymer* 2004, 45, 8211.
- Liu, T.; Tjiu, W. C.; Tong, Y.; He, C.; Goh, S. S.; Chung, T.-S. *J Appl Polym Sci* 2004, 94, 1236.
- Boo, W.-J.; Sun, L.; Warren, G. L.; Moghbelli, E.; Pham, H.; Clearfield, A.; Sue, H.-J. *Polymer* 2007, 48, 1075.
- Zheng, Y.; Zheng, Y. *J Appl Polym Sci* 2006, 99, 2163.
- Nohales, A.; Solar, L.; Porcar, I.; Vallo, C. I.; Gómez, C. M. *Eur Polym J* 2006, 42, 3093.
- Zhou, Y.; Pervin, F.; Biswas, M. A.; Rangari, V. K.; Jeelani, S. *Mater Lett* 2006, 60, 869.
- Usuki, A.; Kawasumi, M.; Kojima, Y.; Okada, A.; Kurauchi, T.; Kamigaito, O. *J Mater Res* 1993, 8, 1174.
- Giannelis, E. P.; Krishnamoorti, R. K.; Manias, E. *Adv Polym Sci* 1998, 138, 107.
- Giannelis, E. P.; Krishnamoorti, R. K.; Manias, E. *Adv Polym Sci* 1999, 118, 108.
- Hackett, E.; Manias, E.; Giannelis, E. P. *J Chem Phys* 1998, 108, 7410.
- Ray, S. S.; Okamoto, M. *Prog Polym Sci* 2003, 28, 1539.
- Enikolopyan, N. S., Ed. *Filled Polymers I: Science and Technology*; Springer-Verlag: Berlin, 1990; Vol. 96.
- de Jayatilaka, A. S. *Fracture of Engineering Brittle Materials*; Applied Science Publishers Ltd.: London, 1979.
- Kuang, W.; Facey, G. A.; Detellier, C.; Casal, B.; Serratos, J. M.; Ruiz-Hitzky, E. *Chem Mater* 2003, 15, 4956.
- Shen, L.; Lin, Y. J.; Du, Q. G.; Zhong, W.; Yang, Y. L. *Polymer* 2005, 46, 5758.
- Solar, L.; Nohales, A.; Muñoz-Espi, R.; López, D.; Gómez, C. M. *J Polym Sci Part B: Polym Phys* 2008, 46, 1837.
- Marcilla, A.; Gomez, A.; Menargues, S.; Ruiz, R. *Polym Degrad Stabil* 2005, 88, 456.
- Tartaglione, G.; Tabuani, D.; Camino, G.; Moisio, M. *Compos Sci Technol* 2008, 68, 451.
- Bokobza, L.; Burr, A.; Garnaud, G.; Perrin, M. Y.; Pagnotta, S. *Polym Int* 2004, 53, 1060.
- Xie, S.; Zhang, S.; Wang, F.; Yang, M.; Séguéla, R.; Lefebvre, J.-M. *Compos Sci Technol* 2007, 67, 2334.
- ASTM Specification D790-93. *Flexural Properties of Unreinforced and Reinforced Plastics and Electrical Insulating Materials Annual Book of ASTM Standards*; ASTM Specification, West Conshohocken, PA, 1993. DOI: 10.1520/D0790-93.